



The Impact of the Guide Vane on the BIWT System for the Distributed Wind Generation in the Urban Area

G.Y. Sim¹, M.A.M. Ariff^{1*}, H.H. Goh², S. N. Ramli³, S.Y. Sim⁴, S.K. Chien⁴

¹Faculty of Electrical and Electronic Engineering,
Universiti Tun Hussein Onn Malaysia, 86400, Batu Pahat, Johor, MALAYSIA

²School of Electrical Engineering,
Guangxi University, Nanning, CHINA

³Faculty of Computer Science and Information Technology,
Universiti Tun Hussein Onn Malaysia, 86400 Batu Pahat, Johor, MALAYSIA

⁴Faculty of Engineering Technology,
Universiti Tun Hussein Onn Malaysia Pagoh Campus, 84600 Panchor, Johor, MALAYSIA

*Corresponding Author

DOI: <https://doi.org/10.30880/ijie.2021.13.02.006>

Received 9 June 2020; Accepted 1 December 2020; Available online 28 February 2021

Abstract: This paper reports a study on the impact of the guide vane on the Building Integrated Wind Turbine (BIWT) system for the distributed wind generation in the urban area. The guide vane is combined with the rotor to concentrate and accelerate the incoming wind to drive the turbine for power generation. The improved BIWT system has several advantages over the conventional BIWT system; it does not require the structural reinforcement of the building because it generates electricity based on the wind pressure acting on the building's wall. Furthermore, the guide vane conceals the rotor from the view of pedestrians to maintain the aesthetic value of the building. The analysis focuses on the installation of the BIWT design at a high-rise building. The study evaluates the wind dynamics characteristic on the building's wall using the computational fluid dynamics (CFD) software. Consequently, the producible power output is estimated based on the wind dynamics characteristic. The effectiveness of the BIWT with the guide vane is evaluated on the actual wind data measured at Kota Kinabalu, Sandakan and Kudat. The result shows that the guide vane increases the producible power output by 129.09%.

Keywords: Building Integrated Wind Turbine (BIWT) system; computational Fluid Dynamic (CFD); Guide vane; High-rise building

1. Introduction

Coal, oil, and gas are accounted for as the most conventional energy resources in today's world. However, these resources are limited. The report shows that coal reserves will be entirely consumed in 200 years, gas reserves will drain away in 70 years, and oil reserves will run out only in 50 years [1]. According to global final energy consumption in 2017, fossil fuels accounted for 79.7% with the share of modern renewables, traditional biomass, and nuclear power at 10.6%, 7.5%, and 2.2%, respectively [2]. Reliable alternative energy resources need to be developed sooner rather than later. Consequently, renewable energy appears to be a stronger candidate to overcome this situation. The development of modern renewable energy is concentrated in four critical domains: power generation, heating and cooling, transport fuels, and rural or off-grid energy services [3]. Recently, various research and technological

development have been conducted to increase the market share of renewable energy. The research and development include the utilization of wind and solar photovoltaic as the replacement for fossil-based energy resources [4].

Between these two renewable energy resources, wind energy is a more attractive solution than solar photovoltaic in terms of its controllability. Moreover, the ratio between energy production and land used for wind energy is better as compared to solar photovoltaic. Thus, it is a more popular option to generate electricity in the urban environment. There are lots of ways to gather wind energy in the urban environment; the BIWT system has a vast potential to bring power generation closer to consumers [5]. Hence, researchers and engineers have actively developed and researched the BIWT system to generate electricity for urban applications.

In order to develop an optimized BIWT system, one needs to study the dynamic characteristic of the wind flow around buildings [6]. CFD is one of the analytical tools to study this behavior. It has been used in various engineering applications such as aircraft, automotive, oil, and gases as well as groundwater flow. In addition, CFD is economical, and it does not require any experimental equipment and time. The performance of the analysis depends on the complexity of the mathematic model of the fluid dynamics around the target [7]. In this paper, CFD is used to analyze the dynamic behavior of wind flow entering the BIWT system. There are two BIWT designs considered in this study: with guide vane and without guide vane. This study compares the dynamic behavior of the wind flow entering these two BIWT designs and analyses their performances in generating energy.

Following this introductory sections, Section 2 discusses the state of art of BIWT system. In Section 3, the method of modelling and performance analysis of BIWT system is discussed. This includes the calculation of input wind velocity, CFD simulation of the wind dynamics on BIWT system as well as estimation of producible power output. Consequently, Section 4 and 5 present the velocity calculation for high-rise building and power estimation of BIWT system respectively. Lastly, Section 6 concludes the main findings of this study.

2. State-of-the-art of BIWT System

In this decade, there is an expansion of large-scale wind turbines in power generation due to significant technologies advancements. Although large scale wind turbines in rural topography and wind farms are presently highly efficient, they have crucial limitations due to the long distance between the wind farms and the urban areas where more than half of global energy demand is consumed. Thus, utilizing wind energy directly in the urban area, getting more interest because it can generate electricity and supply to consumers in the shortest distance. The small scale wind turbine in urban areas is still under active research, and it shows that utilizing this technology has a huge potential in urban power generation [8]. Nevertheless, the challenges to applying this system appear to be related to environmental conditions in the urban area, such as low average wind speed, difficulty in reorienting the power generator based on the direction of wind flow, and high turbulence wind flow triggered by neighboring buildings [9]. To address these challenges, the small-scale wind turbines system with a shrouded mechanism has been reported in [10]. This mechanism accelerates the wind velocity and redirects the wind flow to achieve a better angle of attack to improve the producible power output. Then, a small-scale wind turbine system with “Aeolian roof” is discussed in [5]. The system amplifies the wind velocity, which enables the wind turbine to operate at both low and high wind velocities compare to conventional aerogenerators. In [11], a 3 blade H-Darrieus wind turbine with a horizontal shaft running close and parallel to the roof ridge is discussed. The turbine is mounted between a dual-pitched roof and a diffuser-shaped wall. The researcher in [12] and [13] explains about Omni direction guide vane on the top of the building. The system is installed around the boundary of a cylindrical duct that plays the role of a nozzle to lead the air flows towards the wind turbine. Besides that, an integrated roof wind energy system on the rooftop of the building is discussed in [14]. This system captures the wind flows over the top of the building and guides the funnel accelerated wind to a wind turbine. In [15] and [16], a Savonius like wind turbine enveloped by a diffuser shaped shroud is explained. The rotor is installed on the upstream edge of the building; thus, its input velocity is speeded up by the edge of the building. Although this design improves the performance of the small-scale wind turbine system, its applications require structural reinforcement and modification due to the additional wind pressure that needs to be sustained by the wind turbine mounted on the rooftop. Structural reinforcement and modification may increase the risk of building integrity, and it requires enormous capital expenditure. Thus, a low cost and easy-to-install solution are required to address this challenge.

In [17], a BIWT system is directly installed on the building skin to utilize the wind pressure acting on the building wall. Therefore, strengthening or modification of building structure is not necessary. This system integrates guide vanes to the conventional BIWT system to concentrate and speed up the wind velocity to rotate the generator. The increment in wind velocity increases the delivered power output of the generator. Besides, the guide vane conceals the rotor from the view of pedestrians to avoid aesthetically unpleasant. This BIWT system is an attractive solution to the wind power generation in the urban area. However, the study conducted in [17] does not consider the installation of the system at the standard high-rise building. This consideration is a very critical factor to be considered for the development of wind power generation in the urban area. Properties developers prefer to build high-rise buildings in the urban area due to the cost of land and space limitation. Also, the installation of the BIWT system at a lower atmospheric layer may reduce the power output because the surrounding buildings obstruct the flow path of wind velocity. Thus, the installation of the BIWT system is preferred because it will receive a more stable wind flow.

3. Method of Modelling and Performance Analysis of BIWT System

Fig. 1 shows the BIWT system considered in this study. The system combines the guide vane and Savonius type rotor to generate electricity for the building. It is designed to shroud the building’s wall that is not utilized (e.g. ventilation, natural light, view). The design is modular. Thus, it is easy to attach and detach the system at any existing building. From the figure, it is shown that the guide vane combined with the BIWT system is used to collect and concentrate the incoming wind flows and drive the rotor for power generation. The wind blowing at the building’s wall will have a high static pressure while entering the guide vane. The high static pressure wind will rotate the Savonius type rotor and produce electricity. Consequently, the wind pressure will decrease after it rotates the rotor. The BIWT system considered in this study is installed at a fifteen-story high-rise building. The estimated height of the building is 45 m from the ground. This estimation is based on the definition stated in Emporis Standard [18] and Construction Industry Standard of Malaysia [19]. According to these standards, it is stated that a high-rise building is defined as a building with more than 12 floors [18]. The height for each floor is set to 3 m per story [19].

The flowchart of this study is depicted in Fig. 2. From the figure, the study starts by taking the monthly wind speed data from Malaysia Meteorological Department. The data is taken from three separate locations in Malaysia: Kota Kinabalu, Sandakan, and Kudat. These locations are selected due to their potential for the implementation of distributed generations as it is aligned with Malaysia’s government plan, focuses on electrifying Malaysia’s East Peninsular with renewable energy sources [20]. Due to the limitation of the measuring equipment, the height of the wind speed measurement is taken at 10 m height. Thus, logarithmic law [21] is applied to this data to estimate the wind speed at 45 m height. Consequently, the estimated wind speed data at 45 m height is used as the input parameters for the CFD simulation to analyze the wind dynamics characteristic. The geometry of the BIWT system is modelled using Solidwork software. The wind dynamics characteristic flowing through the BIWT design is simulated using ANSYS software. Then, the increment of the wind speed at the rotor is taken into consideration to estimate the producible power output from the BIWT system [22]. Finally, the result is analyzed and compared with the performance of the BIWT design without the guide vane.

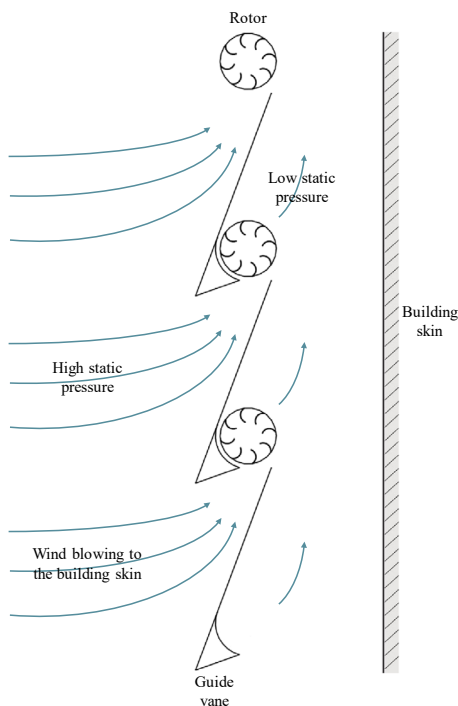


Fig. 1 - The BIWT system with the guide vane

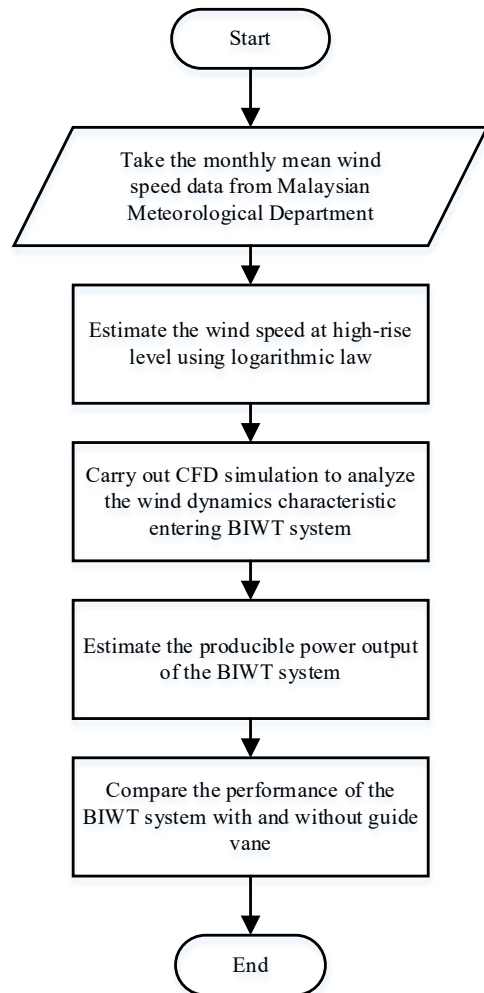


Fig. 2 - Flowchart of study

3.1 Calculating the Input Wind Velocity

The output power of a Savonius rotor depends on the swept area of the rotor. Therefore, the output power of the BIWT system considered in this study also depends on this factor. The larger swept area of the system indicates that more wind is available to create the necessary air pressure against the surface of the rotor to produce the torque and speed required to generate electricity. The swept area depends on the height and the diameter of the rotor blade. It is calculated using (1).

$$A = HD \tag{1}$$

where,

- A = Swept area of rotor
- H = Height of rotor blade
- D = Diameter of rotor

The kinetic energy generated from the BIWT system is calculated using (2). The equation shows that the kinetic energy of the system depends on the mass and the velocity of air passing through the rotor. The mass of air can be estimated based on the air density, the swept area, and the thickness of the air parcel. In the BIWT system design, the swept area can be maximized based on space availability at the installation location. Another option is by maximizing the speed of the air through the rotor blade. This option is realized by using the guide vane in the BIWT design.

$$U = \frac{1}{2}mv^2 = \frac{1}{2}(\rho Ax)v^2 \tag{2}$$

where,

- U = Kinetic energy
- m = Mass of air
- v = wind velocity
- A = Swept area of rotor
- ρ = Air density
- x = Thickness of the parcel

The wind velocity data of Kota Kinabalu, Sandakan, and Kudat are collected at the 10m height. Since the focus of this study is to observe the impact of the guide vane on the BIWT system for the high-rise building. In this study, the altitude chosen to justify the high-rise building application is 45m [18],[19]. Thus, the measured data is modified to suit the scope of this study. This modification is realized by using the logarithmic law to estimate the wind velocity at a different altitude [21]. The wind velocity at 45 m is calculated using (3). From the equation, the surface roughness length for various types of terrain is tabulated in Table 1 [21].

$$v_z = v_{z_r} \cdot \frac{\ln\left(\frac{z}{z_0}\right)}{\ln\left(\frac{z_r}{z_0}\right)} \tag{3}$$

where,

- v_z = Velocity at target height
- v_{z_r} = Velocity at reference height
- z = Target height
- z_r = Reference height
- z_0 = Surface roughness length

Table 1 - Value of surface roughness length for various terrain types

Terrain Description	z_0 (mm)
Very smooth, ice or mud	0.01
Calm open sea	0.20
Blown sea	0.50
Snow surface	3.00
Lawn grass	8.00
Rough pasture	10.00
Fallow field	30.00
Crops	50.00
Few trees	100.00
Many trees, hedges, few buildings	250.00
Forest and woodlands	500.00
Suburbs	1500.00
Centers of cities with tall buildings	3000.00

3.2 CFD Simulation of the Wind Dynamics Characteristic on the BIWT System

This subsection discusses the study of the wind dynamics characteristic at the BIWT system with guide vane using the CFD analysis. First, the BIWT system with the guide vane is model using Solidwork 2018. Then, the model is imported into ANSYS software for CFD analysis. The boundary conditions and the specification requirement need to be set to carry out the analysis. Table 2 shows the boundary condition and specification requirements considered in this study. It is based on the requirements set for a study with similar complexity, as reported in [17]. The CFD analysis is limited only to two-dimensional analysis to minimize the computation time of the simulation. Fig. 3 shows the BIWT system model used in this study. The model is based on the design reported in [17].

From Fig. 3, it is shown that the arrangement of rotors and guide vanes considered in this study. In each module of the BIWT system, the rotors are placed between the guide vane and the building wall. There are three sets of modules overall. The sliding mesh around the rotors is introduced to observe the rotation of the rotor. There are three boundary conditions labeled as "velocity inlet," "wall," and "pressure outlet" are set to carry out the CFD simulation. "Velocity inlet" is imposed at two different places: one at the entrance of guide vane and the other one at the gap in between building skin and lowest guide vane. "Wall" is applied at the back of the assembled modules to represent the role of the building wall. "Pressure outlet" is located at the top edge of the wall surface to allow air ventilation in the system. After completing the CFD simulation, the magnitude of wind velocity is measured at the guide vane outlet point of the highest assembled module with the purpose of producible power estimation.

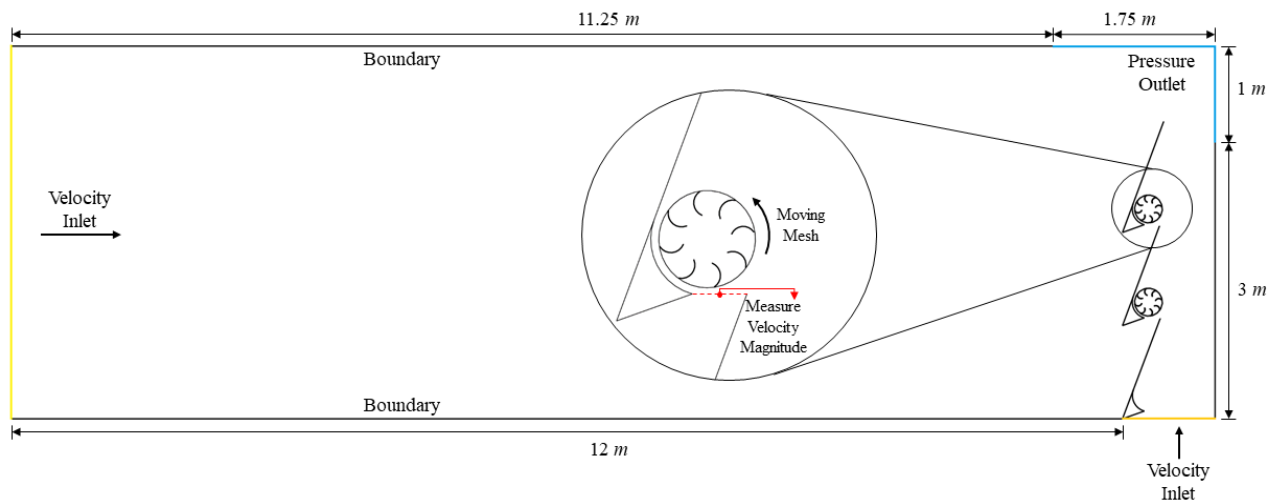


Fig. 3 - BIWT system model for CFD simulation

Table 2 - CFD simulation condition for BIWT system analyses

Computational Conditions	Value
Space	2D
Viscous model	k-omega
Density	1.225 kg/m ³
CFD algorithm	PISO
Interpolating scheme (momentum)	MUSCL
Interpolating scheme (turbulence)	Second order upwind
Inlet/outlet turbulent intensity	10 %
Inlet/outlet hydraulic diameter	1 m
Blade motion type	Moving mesh
Time stepping method	Fixed
Time step size	3.27 × 10 ⁻⁴ s
Number of time steps	720

3.3 Estimating the Producible Power Output

In the CFD simulation, the wind dynamics characteristic is observed, and the wind velocity data is recorded. Based on this data, the power generated P by the BIWT system is formulated from (2). P is defined as the changes in the kinetic energy U with respect to time. Thus, differentiating U in (2) with respect to time equates P , as shown in (4).

$$P = \frac{dU}{dt} = \frac{1}{2} \rho A v^2 \frac{dx}{dt} = \frac{1}{2} \rho A v^3 \quad (4)$$

In an ideal situation, the energy extraction using the BIWT system should be constant. However, it is not the case in practice, as there are always noticeable losses in the system. In the BIWT system, the losses are mainly caused by wind speed reduction over the turbine. In this paper, this discrepancy is modeled by referring to the Betz limit [21]–[23]. Researchers in [21] introduces a power coefficient C_p to represent the efficiency of the wind turbine. According to this study, the highest power coefficient C_p of any wind turbine design operates in an open atmosphere is 0.593. Also, it is considered in this paper. Therefore, equation (4) is reformulated to include the power coefficient, as shown in (5).

$$P_{eff} = \frac{1}{2} \rho A v^3 \cdot C_p \quad (5)$$

4. Velocity Calculation for the High-Rise Building

In order to study the impact of the guide vane on the BIWT system for high-rise buildings, actual wind speed data is collected at various locations. The location considered for this study is Kota Kinabalu, Sandakan, and Kudat in Sabah, Malaysia. The mean of the wind speed data is obtained from the Malaysian Meteorological Department in 2018 from January until December. The measurement is taken at 10 m height. Fig. 4 shows the wind speed data of these three locations.

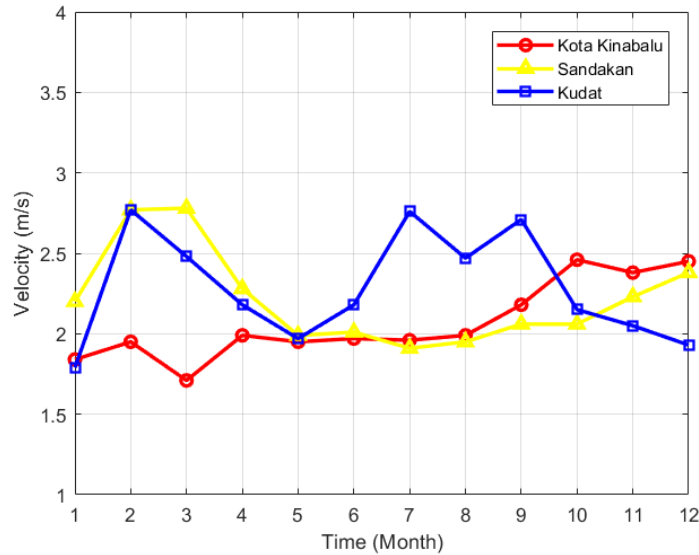


Fig. 4 - Monthly mean wind speed

In Fig. 4, the red, yellow and blue lines represent the wind speed data of Kota Kinabalu, Sandakan and Kudat, respectively. In Kota Kinabalu, the recorded wind speed data increases from 1.84 ms^{-1} in January to 1.95 ms^{-1} in February. However, the speed decreases to 1.71 ms^{-1} in March. Then, the wind velocity increases back to 1.99 ms^{-1} in April and this speed is maintained until August. Consequently, there is a significant increase in September and this increment continues until October. The wind velocity in October is 2.46 ms^{-1} . Finally, the wind velocity data in November and December are 2.38 ms^{-1} and 2.45 ms^{-1} , respectively.

The time-trend of the wind velocity in Sandakan shows different behavior as compared to Kota Kinabalu throughout the year. In January, the wind velocity recorded in Sandakan at 10m height is 2.20 ms^{-1} . Consequently, the wind velocity increased for two consecutive months and peaked at 2.78 ms^{-1} in March. The wind velocity in March is the fastest reading recorded in Sandakan in 2018. Then, the mean wind speed decreases significantly to 2.28 ms^{-1} and 1.99 ms^{-1} in April and May, respectively. In June until October, the wind velocity fluctuates between 1.91 ms^{-1} and 2.06 ms^{-1} . The measurement in July 2018 (1.91 ms^{-1}) is the slowest wind velocity recorded at this location. Finally, the wind velocity time trend shows a slight increment in November and December.

As for the wind velocity in Kudat, the measurement shows a more fluctuation as compared to the other two locations. Kudat experienced three times increment and decrement wind velocity throughout 2018. The increment of the mean wind velocity happened in January until February, May until July, and August until September with 1.79 ms^{-1} to 2.77 ms^{-1} , 1.97 ms^{-1} to 2.76 ms^{-1} and 2.47 ms^{-1} to 2.71 ms^{-1} , respectively. On the other hand, the decrement of the mean wind speed occurs from February until May, July until August, and September until December with 2.77 ms^{-1} to 1.97 ms^{-1} , 2.76 ms^{-1} to 2.47 ms^{-1} and 2.71 ms^{-1} to 1.93 ms^{-1} , respectively. From the figure, the fastest wind velocity recorded in Kudat is in February, while the slowest is in January.

It is discussed in Section 3 that this study focuses on the impact of the guide vane on the BIWT system for a high-rise building. The data obtained from the Meteorological Department is measured at 10m height. Thus, it is necessary to estimate the wind velocity at the 45m altitude based on the measurement at the 10m height. The logarithmic law explained in (3) is applied to the data shown in Fig. 4. Consequently, the estimated wind velocity is tabulated and plotted in Fig. 5. Similar to Fig. 4, the red, yellow, and blue lines represent the wind velocity measurement at Kota Kinabalu, Sandakan, and Kudat. The figure shows a similar time trend with the measured data at the 10m location. The wind velocity at each data point shows a significant increment. However, this increment is not linear as it follows the logarithmic law, as stated in (3). The increment in wind velocity from the 10m and the 45m height is about 225%. This difference is significant; thus, it has to be taken into consideration in order to study the impact of guide vane in the BIWT system for high-rise buildings. However, it is recommended that in the future study, the actual wind velocity at the targeted height is measured directly instead of obtaining it through the estimation process.

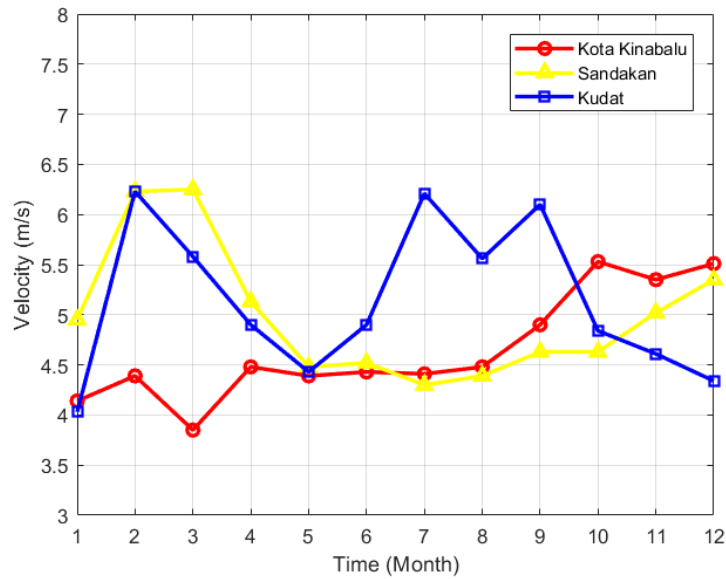


Fig. 5 - Monthly mean wind velocity at 45m

5. Power Estimation of the BIWT System

CFD is a numerical technique to solve the fluid flow problem. It is able to analyze the fluid dynamics characteristic much faster as compared to other methods such as flow filed measurements and wind tunnel experiments with a satisfactory outcome. The CFD analysis is utilized to study the wind dynamics characteristic flowing to the BIWT system with the guide vane installed at the high-rise building. The BIWT system with guide vane, as illustrated in Fig. 6 is imported to the ANSYS software, a CFD simulation tool that is considered in this study. The estimated wind velocity at 45m shown in Fig. 5 is utilized as the boundary conditions. The simulation is conducted with the time-step of 0.327ms for 720 time-steps.

Fig. 6 illustrates the CFD simulation carried out in this study. In this figure, the wind velocity estimated in Fig. 6 is represented as V_i . The wind velocity of interest for this study is at the Savonius rotor V_{con} . This analysis is repeated for every wind velocity data. The wind velocity at the Savonius rotor is recorded for further analysis.

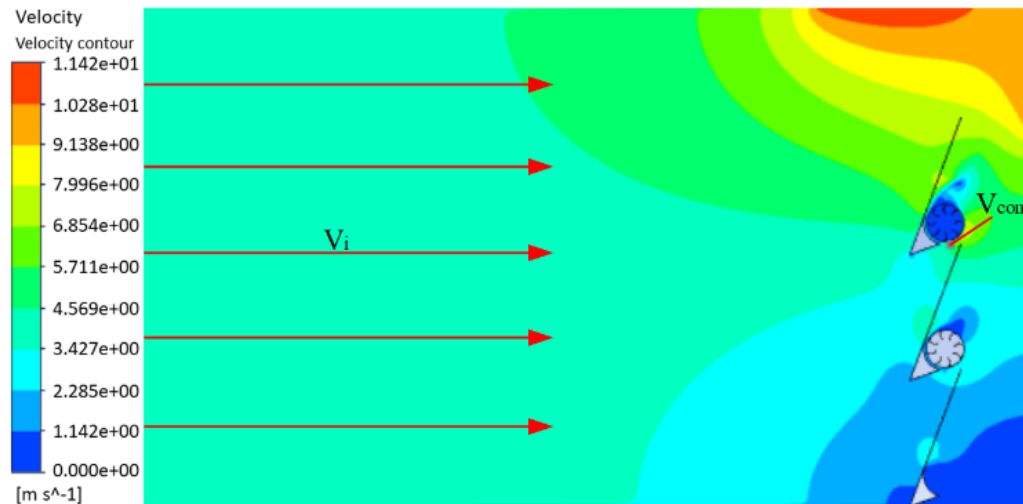


Fig. 6 - CFD simulation of BIWT system

Fig. 7 shows the comparison between the wind velocity at the Savonius rotor for the BIWT system with and without the guide vane. The dashed and solid lines in the graph represent the wind velocity at the Savonius rotor at the BIWT system with and without guide vane, respectively. It is shown in the figure that the levels of wind velocity for both with and without guide vane have a similar time-trend. However, the wind velocity entering the BIWT system with the guide vane is faster as compared to the conventional BIWT system. This observation implies that the guide vane increases the speed of the wind velocity by focusing the flow to the Savonius rotor.

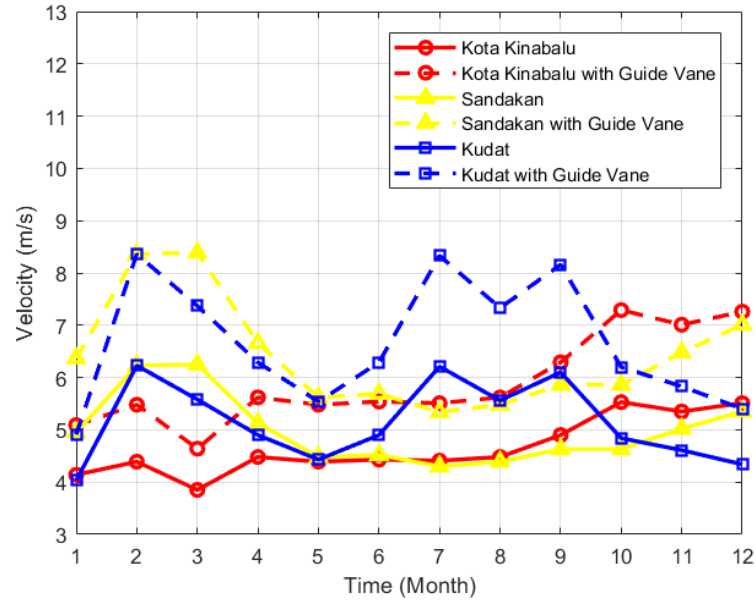


Fig. 7 - Monthly wind velocity with and without guide vane

Table 3 shows the percentage difference of the wind velocity at the Savonius rotor for the BIWT system with and without guide vane for all three locations. From the table, the highest increment in wind velocity at Kota Kinabalu, Sandakan, and Kudat are in October, March, and February, respectively. The most significant impact of the guide vane on the wind velocity is at Sandakan, where the guide vane increases the wind velocity by 34.24% in March. In contrast, the lowest impact of the guide vane is at Kota Kinabalu in March, where the guide vane only increases the wind velocity by 20.52%. The average increment of the wind velocity at Kota Kinabalu, Sandakan, and Kudat is 26.42%, 28.38%, and 29.05%, correspondingly. The result implies that the guide vane increases the wind velocity entering the BIWT system by focusing the wind direction towards the Savonius rotor.

Table 3 - Velocity percentage difference with and without guide vane

Month	Percentage difference (%)		
	Kota Kinabalu	Sandakan	Kudat
January	22.95	28.69	21.84
February	24.83	34.19	34.19
March	20.52	34.24	32.08
April	25.45	29.82	28.37
May	24.83	25.45	25.06
Jun	25.06	25.88	28.37
July	24.94	24.19	34.14
August	25.45	24.83	31.83
September	28.37	26.57	33.77
October	31.83	26.57	28.10
November	31.03	29.08	26.46
December	31.76	31.03	24.42

Fig. 8 represents the producible power output of the BIWT system with and without the guide vane. The result is obtained by applying the simulated wind speed data in Fig. 7 into (4). The dash and solid lines indicate the producible power output of the BIWT system with and without guide vane, respectively. The red, yellow, and blue lines represent the estimated power output for Kota Kinabalu, Sandakan and Sabah, correspondingly. The result shows there is a significant improvement in power output by considering the guide vane in the BIWT system design. The producible power output shown in this study is relatively small because the sizing of the BIWT system is not the scope of this study. The impact of the guide vane on the BIWT system’s power output is highlighted in Table 4.

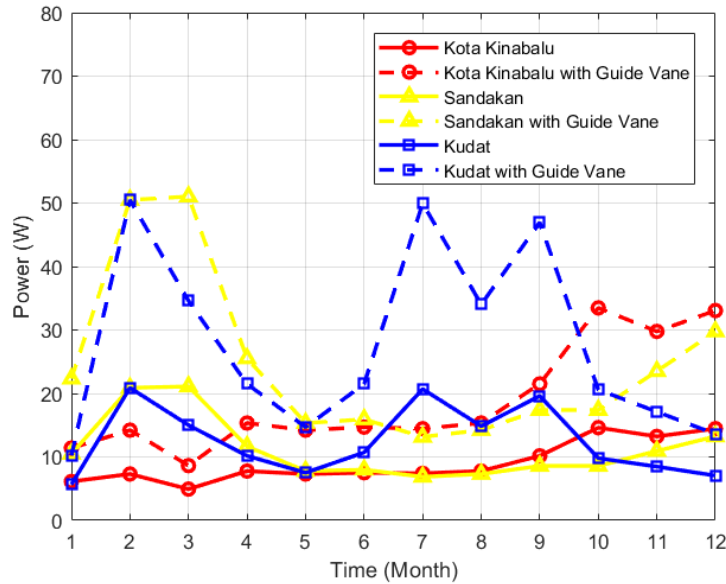


Fig. 8 - Power generated with and without guide vane

Table 4 tabulates the percentage difference in producible power output of the BIWT system with and without the guide vane. It is observed from the table that the highest percentage difference between the BIWT with and without guide vane in Kota Kinabalu, Sandakan, and Kudat is 129.09%, 141.91%, and 141.63%, respectively. This indicates that the installation of the BIWT system with guide vane has the most significant impact in Sandakan. The result tabulated in Table 3 also corroborated this fact, where the highest impact of the guide vane to the increment of the wind velocity is in Sandakan as well. In contrast, the lowest percentage difference between the system with and without guide vane in these three locations is 75.05%, 91.52%, and 80.85%, respectively. This signifies that the guide vane improves the producible power output of the BIWT system by at least 75.05%. Therefore, the impact of the guide vane in the BIWT system design is significant for the application at the high-rise building. The BIWT system with guide vane offers various advantages over other renewable energy generation method, especially in the implementation in the urban areas.

Table 4 - Power percentage difference with and without guide vane

Month	Percentage difference (%)		
	Kota Kinabalu	Sandakan	Kudat
January	85.85	113.11	80.85
February	94.51	141.63	141.63
March	75.05	141.91	130.41
April	97.41	118.81	111.53
May	94.51	97.41	95.58
Jun	95.58	99.49	111.53
July	95.05	91.52	141.36
August	97.41	94.51	129.13
September	111.53	102.74	139.38
October	129.09	102.74	110.20
November	124.95	115.09	102.26
December	128.75	124.95	92.62

6. Conclusion

Conclusively, a study on the impact of the guide vane of the BIWT system is discussed. The study utilized the actual wind velocity data taken at Kota Kinabalu, Sandakan, and Kudat. Then, the wind velocity data at 45m height is estimated based on the actual wind velocity data at 10m height. The estimated wind velocity is utilized as the boundary condition for the CFD analysis of the BIWT system with the guide vane. The wind velocity at the Savonius rotor is recorded to observe the impact of the guide vane to the wind dynamics characteristic entering the BIWT system. Afterward, the producible power output of the BIWT system is estimated based on the wind dynamics characteristic. The result shows that the guide vane increases the wind velocity for at least 20.52% and up to 34.24%. Consequently, the producible power output of the BIWT system increases for at least 75.05%. In addition, the guide vane can increase

the power output by up to 141.91%. The results imply that the guide vane improves the producible power output by focusing the wind flow, hence increasing the wind velocity to rotate the Savonius rotor in the BIWT system for the implementation at the high-rise buildings.

For future study, it is recommended that the sizing of the BIWT system is taken into consideration. Plus, the actual wind velocity measurement at the targeted height should be considered for the implementation of the system at the high-rise buildings.

Acknowledgement

We would like to thank the anonymous reviewer for their valuable comments and suggestion for improvement. Also, we would like to thank the Ministry of Education Malaysia and Universiti Tun Hussein Malaysia for the award of the research grants H304 and H208 that allow this research to be conducted.

References

- [1] Colak, I., Ayaz, M. S., & Boran, K. (2015). CFD based wind assesment in west of Turkey. In 2015 International Conference on Renewable Energy Research and Applications (ICRERA) (pp. 727-731). IEEE
- [2] R. E. N. Members. (2019). Renewables 2019 global status report 2019. France
- [3] M. Brower et al. (2014). Renewables global status report 2014. France
- [4] Kannan, T. S., Mutasher, S. A., & Lau, Y. K. (2013). Design and flow velocity simulation of diffuser augmented wind turbine using CFD. *Journal of Engineering Science and Technology*, 8(4), 372-384
- [5] Carcangiu, S., & Montisci, A. (2012). A building-integrated eolic system for the exploitation of wind energy in urban areas. In 2012 IEEE International Energy Conference and Exhibition (ENERGYCON) (pp. 172-177). IEEE
- [6] Toja-Silva, F., Kono, T., Peralta, C., Lopez-Garcia, O., & Chen, J. (2018). A review of computational fluid dynamics (CFD) simulations of the wind flow around buildings for urban wind energy exploitation. *Journal of Wind Engineering and Industrial Aerodynamics*, 180, 66-87
- [7] Lu, Q., Chen, J., Cheng, J., Qin, N., & Danao, L. A. M. (2011). Study of CFD simulation of a 3-D wind turbine. In 2011 International Conference on Materials for Renewable Energy & Environment (Vol. 1, pp. 596-600). IEEE
- [8] Energy Saving Trust. (2005). Potential for microgeneration: Study and analysis. UK
- [9] Bahaj, A. S., Myers, L., & James, P. A. B. (2007). Urban energy generation: Influence of micro-wind turbine output on electricity consumption in buildings. *Energy and buildings*, 39(2), 154-165
- [10] Müller, G., Jentsch, M. F., & Stoddart, E. (2009). Vertical axis resistance type wind turbines for use in buildings. *Renewable Energy*, 34(5), 1407-1412
- [11] Zanforlin, S., & Letizia, S. (2015). Improving the performance of wind turbines in urban environment by integrating the action of a diffuser with the aerodynamics of the rooftops. *Energy Procedia*, 82, 774-781
- [12] Chong, W. T., Fazlizan, A., Pan, K. C., & Poh, S. C. (2010). Design and wind tunnel testing of a Savonius wind turbine integrated with the omni-direction-guide-vane. In *Proceedings of the Solar Conference* (pp. 211-217)
- [13] Chong, W. T., Fazlizan, A., Poh, S. C., Pan, K. C., Hew, W. P., & Hsiao, F. B. (2013). The design, simulation and testing of an urban vertical axis wind turbine with the omni-direction-guide-vane. *Applied Energy*, 112, 601-609
- [14] Patankar, B., Tyagi, R., Kiss, D., & Suma, A. B. (2016). Evaluation of an integrated roof wind energy system for urban environments. In *Journal of Physics: Conference Series* (Vol. 753, No. 10, p. 102007). IOP Publishing
- [15] Krishnan, A., & Paraschivoiu, M. (2016). 3D analysis of building mounted VAWT with diffuser shaped shroud. *Sustainable Cities and Society*, 27, 160-166
- [16] Larin, P., Paraschivoiu, M., & Aygun, C. (2016). CFD based synergistic analysis of wind turbines for roof mounted integration. *Journal of Wind Engineering and Industrial Aerodynamics*, 156, 1-13
- [17] Park, J., Jung, H. J., Lee, S. W., & Park, J. (2015). A new building-integrated wind turbine system utilizing the building. *Energies*, 8(10), 11846-11870
- [18] Nizamani, Z., Thang, K. C., Haider, B., & Shariff, M. (2018). Wind load effects on high rise buildings in Peninsular Malaysia. In *IOP Conference Series: Earth and Environmental Science* (Vol. 140, No. 1, p. 012125). IOP Publishing
- [19] L. P. I. P. Malaysia. (2010). Construction Industry Standard, vol. CIS 18. Malaysia
- [20] G. Heartbeat, L. Term, and E. Security. (2017). *Energy in Malaysia: Towards a brighter future*. Energy Commission, vol. 12, Malaysia
- [21] Manwell, J. F., McGowan, J. G., & Rogers, A. L. (2010). *Wind energy explained: theory, design and application*. John Wiley & Sons
- [22] Schubel, P. J., & Crossley, R. J. (2012). Wind turbine blade design. *Energies*, 5(9), 3425-3449
- [23] Mathew, S. (2006). *Wind energy: fundamentals, resource analysis and economics*. Springer